Final Report of the $\bar{\text{P}}$ANDA PID TAG

Draft 0.2

G. Schepers, GSI Darmstadt

Contents

1 Introduction **4**

2 Physics Requirements **5**

3 Tools **5**

3.1 Separation Power 6

3.2 Phase space plots 6

3.3 Fast Simulation 6

4 PID Subsystems **6**

4.1 Tracker 7

4.1.1 Time Projection Chamber (TPC) 7

4.1.2 Straw Tube Tracker (STT) 7

4.2 Time of Flight (ToF) 7

4.3 Barrel DIRC 7

4.4 Barrel Calorimeter 8

4.5 Forward Cherenkov 8

4.5.1 Focusing Disc DIRC 8

4.5.2 Time of Propagation Disc DIRC 10

4.5.3 Proximity RICH 11

4.5.4 Forward RICH 12

4.6 Forward Calorimeter 12

4.7 Muon Counter 12

5 Evaluation **12**

5.1 Potential of the Subsystems 12

5.2 Matching of the Subsystems 12

6 Global PID Scheme **12**

7 Optimized Set of Detectors and Parameters **13**

8 Conclusion **13**

9 Acknowledgments **13**

10 Appendix **13**

1 Introduction

The $\bar{\text{P}}$ANDA ([1]) PID TAG (Particle Identification Technical Assessment Group) was installed to give a recommendation to the collaboration about an optimal set of particle detectors. The task given to this TAG is described in more detail:

Subject

- Requirements from physics
- Evaluate potential of each subsystem
- Matching of systems

Deliverables

- Definition of global PID scheme
- Optimized set of detectors and parameters

This list reflects roughly the structure of the PID TAG work and of this report. In an additional subsection the tools available for the PID TAG work are presented and explained (see also [2]) . The PID TAG evaluated the necessity of mapping the "Separation Power" in dependence of the momentum and the polar angle of the reaction products which is described in section 3.1. Since a "full simulation" was not available to calculate the performance of all the sub detectors, the TAG gathered parameterizations of the single sub detectors which went into a "Fast Simulation" explained in section 3.3. For single physics channels a "Full Simulation" was used.

Amongst others some important questions to solve were:

- Do we need the PID information of a Time Projection Chamber (TPC)? If, not, it is also on the Tacking TAG to give recommendations for eather the TPC of a Straw Tube Tracker (STT).
- Do we need a Froward Cherenkov? If, yes, of which form? The PID TAG compared two design studies of Disc DIRCs which differ in the method of read out and in addition a possible solution with a Proximity RICH.
- Do we need a Forward RICH?

The PID TAG had about 10 presence meetings and over 15 on line meetings. First PID subsystems were defined. Each subsystem has its responsible representative. Each representative had a replacement of his own group to guarantee always the same level of knowledge in all subsystems. For special subjects experts were asked to present informations in the meeting or to give answers to questions which arose.

The members of the TAG and their special responsibilities are listed at the end of the document (section 10).

2 Physics Requirements

The HESR (High Energy Storage Ring) of the new FAIR (Facility for Anti proton and Ion Research) project provides an Anti proton beam of high resolution (down to $\Delta p = 1 \times 10^{-5}$) and intensity from 1.5 GeV/c to 15 GeV/c momentum.

This offers the unique possibility of investigating a broad filed of physics. The vast variety of reaction types from meson-production over Charmonium decays to Hyper nuclear reactions demands a complete and compact detector system.

The physics requirements to the detectors are:

- to cover the full angular range of the physics products
- to detect all momenta of the reaction products
- to separate particle types with a defined level of separation over the full range of momenta of the reaction products.

The full solid angle can only be covered by the full set of detectors. Sometimes the momentum coverage has to be fulfilled by a combination of two or even three sub detectors.

For the single subsystems benchmark-channels had to be identified (Table 1) and simulated.

Channel	Final state	Related to detector
$\bar{p}p \to (n)\pi^+\pi^-$	$(n)\pi^+\pi^-$	EMC
$\bar{p}p \to \psi(3770) \to D^+D^-$	$2K\,4\pi$	DIRCs, ToF
$\bar{p}p \to \eta_c \to \phi\phi$	4K	DIRCs
$\bar{p}p \to D_S D^*_{S0}(2317)$	$\pi^\pm K^+ K^-$	DIRCs
		muon
		Forward RICH

Table 1: Benchmark channels to evaluate the performance of the different PID detectors.

At $\bar{\text{P}}$ANDA 2×10^7 reactions per second with up to 10 charged particles per reaction have to be digested by the detectors.

3 Tools

In this section the TAG work is described. To evaluate the performance of the detectors the PID TAG defined the "Separation Power" as the right tool (see section 3.1. With the help "Phase Space Plots" (section 3.2)the angular coverage and the corresponding particle momenta could be determined. The "Fast Simulation" (section 3.3) was used to map the separation power over the full angular and momentum range. In a second step important reactions and their relevant background channels were simulated. Thus the regions where a good separation power is needed could be identified and checked whether the detector performance is sufficient there.

3.1 Separation Power

The PID TAG decided to use the separation power with the sigma separation value defined as

$$\sigma_{sep} = \frac{|m_A - m_B|}{\sigma_\beta} = \frac{|m_A - m_B|}{(\sigma_A/2 + \sigma_B/2)}$$

where A and B are two different particle types of the same momentum. The masses m_A, respectively, m_B are Gauss distributed with the σ being the standard deviation.

The particle flux (so different amplitudes of the distributions) was not taken into account as well as different width or even shapes of the distributions. Nevertheless this definition can give a qualitative measure to the detector performance needed for their evaluation. In the calculation with the Fast Simulation the definition of the separation power, however, varied slightly, allowing different widths of the Gaussian distributions of both particles (3.3).

3.2 Phase space plots

Following a request of the PID TAG phase space plots from all the reactions relevant for the physics book were produced. The set of plots shows for each particle species of the reaction the particle momentum versus theta angle and the transversal versus the longitudinal momentum.

3.3 Fast Simulation

In order to get information about phase space (.i.e. momentum-theta dependence) coverage of the different PID relevant subsystems maps of separation power have been generated based on fast simulations of single track events, i.e. the particles properties are modified with an effective parametrization of detectors responses and PID information is estimated and attached to the resulting particle candidate. Since no microscopic simulation is performed and no exact geometry information is taken into account, the accuracy of this approach is limited, the computation time on the other hand is orders of magnitude shorter offering the possibility to do studies with higher statistics.

4 PID Subsystems

The different behavior of charged particles traversing active and passive detector material can be used to identify (on a probabilistic level) the nature of a charged particle. The PID detectors used in PANDA take advantage of the following effects:

- Specific Energy Loss. The mean energy loss of charged particles per unit length, usually referred to as dE/dx, is described by the Bethe-Bloch equation which depends on the velocity rather than momentum of the charged particle.
- Cherenkov Effect. Charged particles in a medium with refractive index n propagating with velocity $\beta > 1/n$ emit radiation at an angle $\Theta_C = arccos(1/n\beta)$. Thus, the mass of the

detected particle can be determined by combining the velocity information determined from Θ_C with momentum information from the tracking detectors.

- Time-of-flight. Particles with the same momentum, but different masses travel with different velocities, thus reaching a time-of-flight counter at different times relative to a common start.
- Absorption. A thick layer of passive material absorb most particles due to electromagnetic (e+e-, γ) or hadronic interactions (all charged and neutral hadrons). After a certain amount of material only muons and neutrinos survive. The muons can then be detected easily with any kind of charged particle detector, depending on the desired speed and resolution.

The group of subsystems building the particle identification system of $\bar{\text{P}}$ANDA are listed with growing distance to the Target point:

- Time Projection Chamber
- Time of Flight
- Barrel DIRC
- Barrel Calorimeter
- Forward Cherenkov
- Forward Calorimeter
- Muon Counter

4.1 Tracker

4.1.1 Time Projection Chamber (TPC)

4.1.2 Straw Tube Tracker (STT)

4.2 Time of Flight (ToF)

4.3 Barrel DIRC

The purpose of the Barrel DIRC (Detection of Internal Reflected Cherenkov photons) is to provide a positive kaon identification. This can be achieve with the determination of the mass of the particle by combining the velocity information of the DIRC with momentum information from the tracking detectors. In addition the distinction of gammas and relativistic charged particles entering the EMC behind the DIRC is possible.

Basis for the calculations and simulations are the bar dimensions taken from the BaBar DIRC [3]. With the length adapted to the $\bar{\text{P}}$ANDA setup there are quartz bars of $17 \times 35 \times 2300$ mm^3 and a distance of 480 mm to the target point. Thus the barrel DIRC covers the solid angle of 22 to 140 degrees. The lower momentum threshold for kaons which produce Cherenkov light is for an envisaged refractive index of n=1.47 as low as 460 MeV?/c for single photon production. For photon numbers bigger than 4 (necessary for the reconstructions of the "Cherenkov rings")it is more than 200 MeV?/c higher.

With 17mm (of thickness) of fused silica the DIRC bars present approximately 14% of a radiation length to normal incident particles. The support structure will add some more percent.

This design is initially based on the BaBar DIRC [3] but at P̄ANDA further improvements of the performance are under development. The combination of the spacial image of the photons with their time of arrival gives access not only to their velocity but also to the wavelength of the photons. Thus dispersion correction at the lower and upper detection threshold becomes possible. Further on the reduction of the photon readout in size and number of photon detectors is envisaged. A lens or a set of lenses at the exit of the quartz bar focus the photons to a focal plane behind a readout volume of about 40 cm length. When this volume is filled with a medium with the same refractive index as the radiator material (n_{medium}=$n_{radiator}$=1.5) additional dispersion effects are avoided.

4.4 Barrel Calorimeter

4.5 Forward Cherenkov

Two DIRC design options exist for the endcap part of the target spectrometer section. These differ in the photon readout design but both use an amorphous fused silica radiator disc. The endcap detector position covers forward angles of up to $\vartheta = 22°$ excluding an inner rectangular area of $\vartheta_x = 10°$ horizontal and $\vartheta_y = 5°$ vertical half-angles. Simulations using the DPM generator [4] give 1.0±0.8 (at 2 GeV/c) to 2.3±1.8 (at 15 GeV/c) charged particle multiplicity per $\bar{p}p$ interaction emitted from the target vertex into this acceptance.

In such a one-dimensional[1] DIRC type, a photon is transported to the edge of a circular disc while preserving the angle information. Avoiding too much light scattering loss at the surface reflections requires locally (in the order of millimeters) a surface roughness not exceeding several nanometers RMS.

The lower velocity threshold, which is common to both designs, depends on the onset of total internal reflection for a part of the photons emitted in the Cherenkov cone.

4.5.1 Focusing Disc DIRC

In the Focusing Light guide Dispersion-Correcting design (Figures 1 and 2), when a photon arrives at the edge of the circular or polygonal disc, it enters into one of about hundred optical elements on the rim. Here the two-fold angular ambiguity (up-down) is lifted, the chromatic dispersion corrected and the photon focused onto a readout plane. While the optical element entered determines the ϕ coordinate, measuring the position in the dispersive direction on the focal plane of the focusing light guide yields the θ coordinate.

Lithium fluoride (LiF) is UV transparent and has particularly low dispersion. Proton beam irradiation of a test sample shows that radiation-produced color centers are confined to sufficiently

[1] Light is only reflected on surfaces of one spatial orientation, here the two disc surfaces both normal to the z axis.

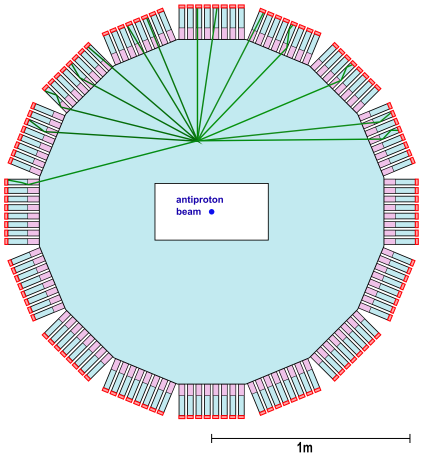

Figure 1: Polygonal disc with focusing light guides attached to the rim used as optical readout components.

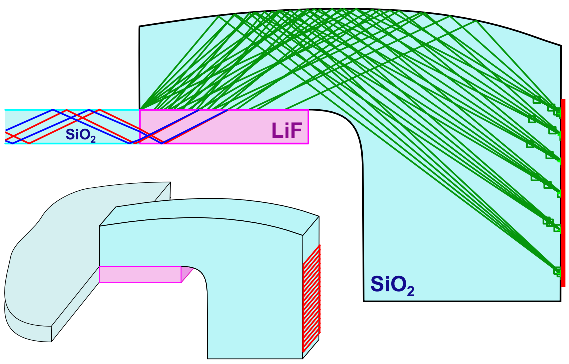

Figure 2: Light guide side view (inset 3D-visualisation) shown with a set of rays used for optimising the light guide curvature. Reflections at the parallel front and back surfaces keep the light inside but do not affect the focusing properties.

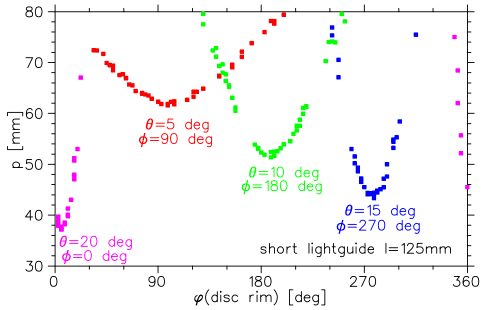

Figure 3: Simulated photon hit pattern for four particles emitted at different angles θ and ϕ from the target vertex.

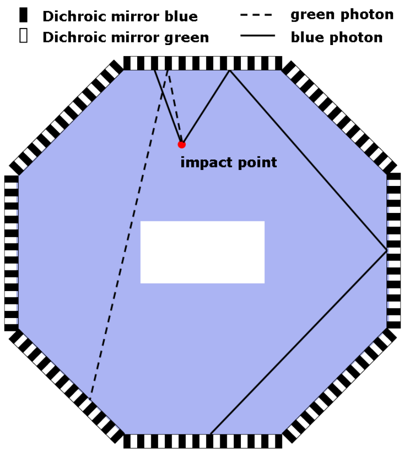

Figure 4: Sketch of the flightpath in the ToP Disc

small wavelength ranges, and are only partially absorbing at the expected $\bar{\text{P}}$ANDA lifetime dose. Hence we believe we can use LiF as a prism element (see Fig. 2) to correct the Cherenkov radiation dispersion. The two boundary surfaces, with the radiator disc and the subsequent light guide, make the chromatic dispersion correction angle-independent to first order.

As with the radiator, the light impinging on the inside of the light guide's curved surface undergoes total internal reflection, hence no mirror coating is needed. This reflection makes the focusing also independent of the wavelength.

With the light staying within the dense optical material of the light guide, most of the incoming light phase space from the disc is mapped onto the focal plane with its one-coordinate readout. The focusing surface with cylindrical shape of varying curvature has been optimised to give an overall minimum for the focus spot sizes of the different angles on the focal plane, individual standard deviations being well below 1 mm for the instrumented area.

4.5.2 Time of Propagation Disc DIRC

In the Multi-Chromatic Time-of-Propagation design ([5]) small detectors measure the arrival time of photons on the disc rim, requiring σ_t=30–50 ps single photon time resolution. For any given wavelength, the disc edge is effectively covered alternately with mirrors and detectors. Only due to the resulting different light path-lengths one can determine accurately enough the start reference time, i.e. the time when the initial charged particle enters the radiator, as the stored anti proton beam in the HESR has no suitable time structure to be used as an external time start.

As some of the light is reflected several times before hitting a detector, the longer path lengths allow a better relative time resolution.

The use of dicroic mirrors as color filters allows the use of multiple wavelength bands within the same radiator (the current design suggesting two bands) resulting in higher photon statistics. The narrow wavelength bands minimise the dispersion effects, and the quantum efficiency curve of the photo cathode material could be optimised for each wavelength band individually.

4.5.3 Proximity RICH

As alternative approaches Proximity Imaging Solutions were considered.

- Liquid radiator proximity RICH using CsI GEMs: Proximity focusing RICH detectors use the most simplest imaging geometry. Their resolution depends on the optical quality and crucially on the ratio of radiator thickness to stand-off distance, the distance between the creation and detection of the photon. Using liquid or solid radiators yielding enough Cherenkov photons, the radiator can be kept rather slim, which in turn only require moderate stand-off distances on the order of 100 mm. The ALICE HMPID detector is build in this fashion using a C6F14 liquid radiator and CsI-photon cathodes in an MWPC. This requires a UV optic. It is proposed to use the same radiator technique and combine the third tracking station with a CsI coated GEM photon detector. The detector will be thicker along the beam direction than the DIRC detector previously described, but can be essentially moved to any position along the beam axis. The estimated performance and the ALICE/STAR test results show a significant decrease in performance compared to the DIRC solutions.

- Solid radiator proximity RICH using CsI GEMs: One of the main drawbacks of using the ALICE design is the use of C6F14. This radiator is rather sensitive to impurities and radiation damage requiring a purification system. Using a fused silica disc with a properly machined surface as radiator circumvents the problem while keeping the geometrical advantages of the design. Initial studies show a further reduction of performance mainly due to strong dispersive effects in the UV region.

- Aerogel proximity RICH using PMTs: The Belle endcap Cherenkov threshold counter will be replaced by a proximity imaging RICH counter using an Aerogel radiator and conventional BiAlkali based multi-pixel PMTs as photon detectors. Using a so-called focusing radiator scheme, prototypes show excellent performances. The main technological challenge for this detector is to realise a photon detection matrix in a strong magnetic field. Recent developments in the field of proximity focusing HAPDs seem to make such a detector realistic. The large number of pixels required should the detector be placed behind the EMC, but inside the cryostat merit a detailed look at the costs of such a design.

4.5.4 Forward RICH

4.6 Forward Calorimeter

4.7 Muon Counter

5 Evaluation

Parametrization of the Barrel DIRC: Following the Particle Data Group [[6]] the resolution of the track Cherenkov angle σ_{track} scales with the square root of the number of photons detected:

$$\sigma_{track}(\Theta) = \frac{\sigma_{single}(\Theta)}{\sqrt{N_{ph}}} \tag{1}$$

The Θ-dependence comes from the fact that the path length in the detector material varies with the particle angle which is directly proportional to the number N of produced Cherenkov photons.

Thus we find approximatively the separation of two particle species, i.e. numbers of σ (N(σ)), with masses m_1 and m_2, which pass a radiator of the refraction index n with the momentum p:

$$N(\sigma) \ = \frac{|m_1^2 - m_2^2|}{2p^2\sigma_{track}(\Theta)\sqrt{n^2-1}} \tag{2}$$

To provide useful results the DIRC should produce 15 to 20 photons per particle track. The correlation calculated with a photon number of 16 is shown in the figure bellow.

A further effect which is very important and specific for DIRC detectors is the caption probability of the produced light cone from the Cherenkov photons. Depending again on the angle Θ of the incoming particle only a fraction of the photons fulfill the conditions for total internal reflection. The rest gets lost from the radiator before the first reflection. All known effects are included in the Fast Simulation (3.3)

5.1 Potential of the Subsystems

5.2 Matching of the Subsystems

6 Global PID Scheme

The PANDA spectrometer will feature a complete set of innovative detectors for particle identification. The detection of neutral particles will be performed by a highly granular electromagnetic calorimeter. Charged particles will be identified in the low momentum region by their energy deposit and ToF, in all other momentum regions by innovative DIRC detectors. The target spectrometer will be complemented by a forward spectrometer to detect high momentum particles and surrounding muon detectors. Each detector systems performance is optimised in itself. Studies have begun to combine the responses of various detectors in a common framework based on a likelihood scheme or a carefully trained neutral network. These combined likelihood schemes are successfully employed at various detector systems like HERMEs, Belle and BaBar. They rely on a reliable parametrisation of the detector component response from simulation and test-beams. This has to be taken into account in testing PANDA's individual components. The combined performance of the system will be significantly better than the individual separation powers.

7 Optimized Set of Detectors and Parameters

8 Conclusion

9 Acknowledgments

Thanks to analyzers from the "$\bar{\text{P}}$ANDA Physics Book", and all who help with their work and expertise to the success of the PID TAG.

This work is supported by EU FP6 grant, contract number 515873, DIRACsecondary-Beams.

References

[1] $\bar{\text{P}}$ANDA Collaboration, Technical Progress Report, FAIR-ESAC/Pbar 2005

[2] http://panda-wiki.gsi.de/cgi-bin/viewauth/Tagpid/WebHome, Wiki page of the $\bar{\text{P}}$ANDA PID TAG

[3] R. Aleksan et al., Nucl. Inst. Meth. **A397**, 261 (1997)

[4] A. Galoyan, V.V. Uzhinsky, AIP Conf. Proc. 796, pp. 79-82, 2005

[5] P. Schönmeier et al., to appear in the proceedings of 6th International Workshop on Ring Imaging Cherenkov Counters (RICH 2007), Trieste, Italy, 15-20 Oct 2007.

[6] W.-M. Yao et al. 2006 J. Phys. G: Nucl. Part. Phys. **33** 1

10 Appendix

Members of the PID TAG

- G. Schepers, C. Schwarz - Barrel Dirc (Chairs)
- B. Kopf, R. Novotny - Barrel Calorimeter
- B. Seitz - Cherenkov Counter (Global PID)
- O. Denisov / M. P. Bussa - Muon Counter
- K. Föhl / P. Vlasov - Forward Cherenkov

- J. Smyrski / O. Wronska - Forward Calorimeter
- Q. Weitzel / S. Neubert - Time Pjection Chamber
- C. Schwarz, A. Galoyan - Time of Flight
- K. Götzen - Fast Simulation
- K. Peters - Physics